

COB-2023-1611

Experimental assessment of piezoelectric energy harvesting from VIV on cantilevered flexible cylinders with orthotropic bending stiffness

Leticia S. Madi¹

Wagner A. Defensor Filho¹

1 – Offshore Mechanics Laboratory (LMO), Escola Politécnica, Universidade de São Paulo, Brazil
leticia.madi@usp.br; wadfilho@usp.br

Guilherme J. Vernizzi¹

guilherme.jorge.lopes@usp.br

Andre M. Kogishi²

2 – Institute for Technological Research (IPT), São Paulo, Brazil
amkogishi@ipt.br

Celso P. Pesce¹

ceppesce@usp.br

Abstract. Vortex-induced vibrations (VIV) is a phenomenon characterized by self-excited oscillations which can be exploited for low-power energy harvesting. In this experimental study, an orthotropically stiffened cantilevered cylinder with piezoceramic components is used to convert vibratory energy into electrical energy, exploring the high-energy branch observed in VIV experiments with this particular configuration. The experiments were conducted at the IPT towing tank, for various constant towing velocities until reaching a steady state. Reduced velocities up to $Ur = 20$ were attained, allowing exploration of various VIV frequencies and response branches. Measurements included the electric tension output of the piezoelectric circuits and cylinder displacements tracked through an optical system. This proof-of-concept study lays the groundwork for potential applications of VIV energy harvesting from this specific configuration and provides valuable insights for future optimizations.

Keywords: flow-induced vibration, piezoelectric energy harvesting, Vortex-Induced Vibration, experimental analysis, orthotropic stiffness

1. INTRODUCTION

Vortex-induced vibration (VIV) is a resonant fluid-structure interaction resulting from alternated vortex shedding on bluff bodies exposed to a fluid stream, inducing oscillatory lift forces. When the frequency of vortex shedding, and thus the oscillatory forces, aligns with a natural frequency of the system, a synchronization phenomenon known as lock-in occurs. For a cylinder with a diameter D exposed to a flow velocity U , relevant parameters for describing this phenomenon are detailed in Tab. 1. The relationship between vortex shedding frequency (f_s) and flow velocity is denoted by the Strouhal number (St). The parameter reduced velocity (Ur) characterizes the flow velocity in terms of the vortex shedding frequency and the structural natural frequency (f_n). Given that the expected amplitudes of movement in VIV are on the order of the cylinder diameter, the dimensionless amplitude A^* is defined. More in-depth description and analysis of VIV on elastically mounted cylinders can be found, for example, in Khalak and Williamson (1999), Sarpkaya (2004) and Williamson and Govardhan (2004).

Table 1. Dimensionless parameters related to the VIV phenomenon.

Parameter	Symbol	Definition
Strouhal number	St	$f_s \frac{D}{U}$
Reduced velocity	Ur	$\frac{U}{f_n D} = \frac{f_s}{f_n St}$
Dimensionless amplitude	A^*	$\frac{A}{D}$

1.1 VIV energy harvesting

Due to its vibratory nature, VIV is extensively studied in engineering due to its impact on fatigue analysis. However, the phenomenon can be approached from an alternative perspective, in the context of energy harvesting. A pioneer device using such concept is the VIVACE, a medium power device based on a series of cylinders arranged in tandem, coupled to electromagnetic transducers (for further detail on the VIVACE, see Bernitsas *et al.* (2006); Sun *et al.* (2017)). Given the increasing use of portable electronic devices and the demand for advanced battery technologies and energy storage, exploring energy harvesting from VIV becomes an interesting approach (see Han *et al.* (2023)). This phenomenon is characterized by self-excited and self-limited oscillations, allowing for controlled vibrations that can be converted into electrical energy. Such a harvester proves particularly useful for low-power requirements in self-reliant electronic devices like remote sensors. A commonly used method for the conversion of mechanical energy into electricity is the use of piezoelectric transducers. Other harvesters based on the VIV phenomenon with piezoelectric conversion can be found in Song *et al.* (2015), Shan *et al.* (2017), Han *et al.* (2020) and Zhao *et al.* (2022).

1.2 VIV on orthotropically stiffened cylinders

In the distinct case of VIV on a flexible cantilevered cylinder with a flat bar providing higher stiffness in the flow direction than transversally, a unique dynamic response branch is observed at high reduced velocities, as first seen by Fujarra *et al.* (2001). Contrary to the expected desynchronization, a high energy branch is observed, highlighted in Fig. 1. As confirmed by the experiments in Defensor Fo. *et al.* (2022), this branch remains stable even at high income flow velocities, presenting a rich spectrum of frequencies in its multimodal response for arrangements with various ratios between transverse and longitudinal resonant frequencies ($f^* = f_x : f_y$). Figure 2 presents amplitude and frequency spectra for a model with frequency ratio $f^* = 2 : 1$, evidencing the high-energy branch for this kind of structure. Based on the previous studies, an energy harvester is proposed to harness the high frequencies exhibited by this particular branch.

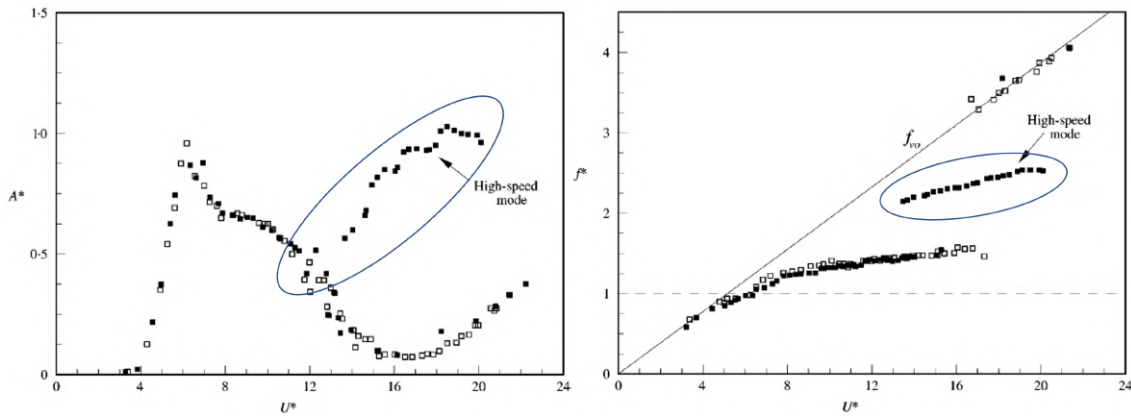


Figure 1. VIV response for orthotropic stiffened flexible cantilevered cylinder of $f^* = 4 : 1$: cross-wise amplitudes and frequency of vibration as functions of reduced velocity. (Fujarra *et al.*, 2001). High energy branch highlighted.

This study involves the experimental analysis of an orthotropically stiffened cantilevered cylinder with piezoceramic components installed on the flat bar to convert vibratory energy into electricity. The focus is on the proof of concept rather than optimizing the energy conversion system. The experimental set-up and methodology of the tests are described in Sec. 2, while Sec. 3 discusses the data analysis methodology and results obtained. Concluding remarks on this ongoing study are presented in Sec. 4.

2. EXPERIMENTAL SET-UP

The experiments in this research aim to assess the feasibility of utilizing the high frequencies of the high-energy branch for energy harvesting using piezoelectric transducers. The investigated model consists of a cantilevered standard PVC pipe of length $L = 2.0$ m and external diameter $D = 40$ mm, with an arrangement of internal flat bars to establish varying stiffness in orthogonal directions. Piezoelectric layers are attached to the polymeric beams at the clamped end, one on each side. These piezoelectric beams are ready-to-use macro fiber composites (MFC) from Smart Material Corporation®, comprising aligned piezoceramic fibers sealed with epoxy adhesive and a polymeric film, connected to electrodes. Each MFC is linked to a simple electrical circuit with only an electric resistance of $R = 270$ k Ω in parallel. Figure 3 depicts the orthotropically stiffened cantilever and the MFC patch attached in its interior. Relevant parameters for the experiments are presented in Tab. 2.

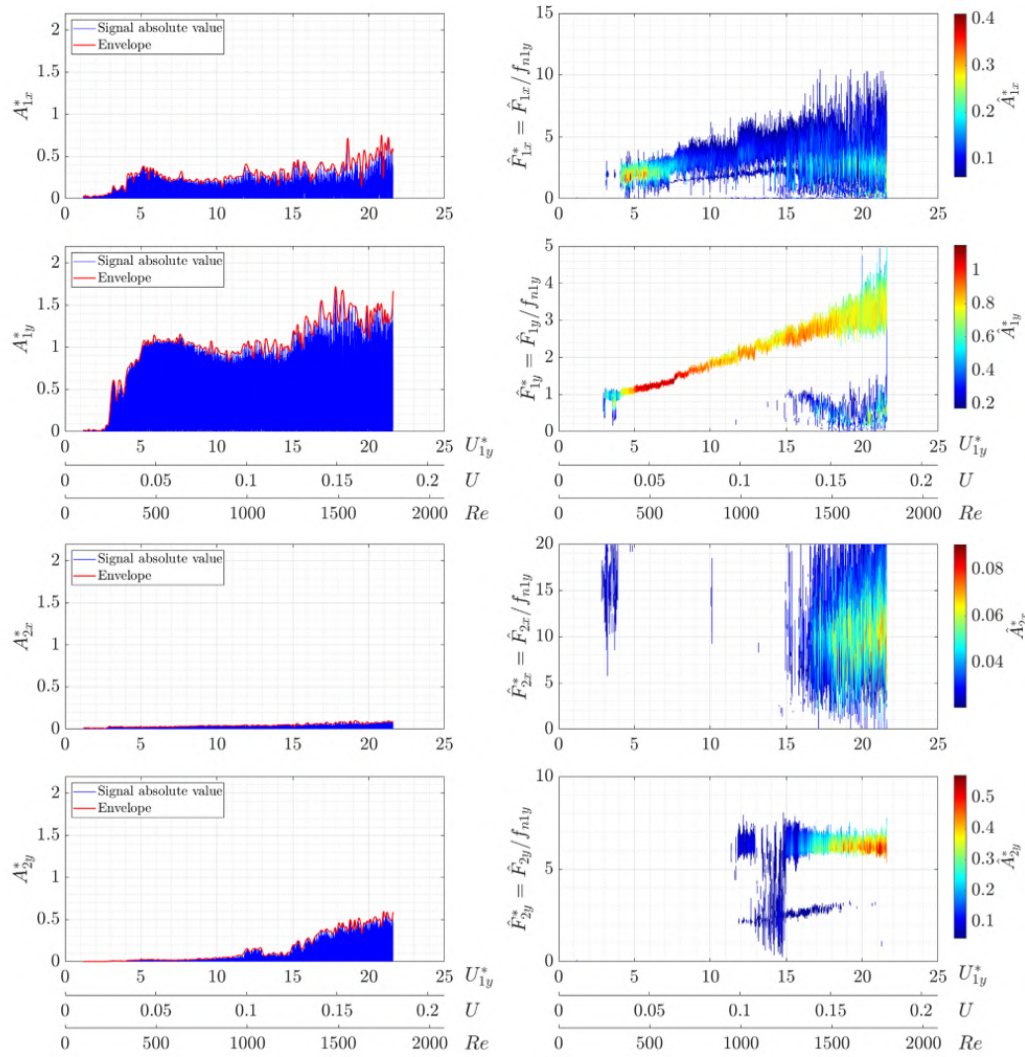


Figure 2. Modal VIV response branches for orthotropic stiffened flexible cantilevered cylinder: in-line and cross-wise Dimensionless modal amplitudes and dimensionless modal frequencies as functions of reduced velocity. Model nominal frequency ratio $f^* = 2 : 1$ (Defensor Fo. *et al.*, 2022).



Figure 3. Constitution of the experimental model. Cantilevered structure and reflective targets (left), MFC beam attached to the model and electric circuit (right).

Table 2. Parameters related to the experimental model

Structural parameters		Natural frequencies	
Length (L)	2.0 m	1st Longitudinal natural frequency (f_{x1})	2.34 Hz
Diameter (D)	40 mm	1st Transversal natural frequency (f_{y1})	1.32 Hz
Electrical resistance (R)	270 k Ω	2nd Transversal natural frequency (f_{y2})	8.30 Hz
		Frequency ratio (f_{x1}/f_{y1})	1.77

The tests were conducted at the towing tank of the Institute for Technological Research (IPT). The displacements were directly measured using Qualysis® optical tracking system, which collected data from the reflective targets placed at equally spaced intervals along the model. Figure 4 illustrates the experimental setup of the camera system and the experimental model attached to the towing car. The electric tension output of the piezoelectric circuits is also acquired. A set of testing velocities was defined, for which the car was towed until reaching a steady state¹ response. The towing velocities vary from $U = 0.1$ m/s to $U = 1.0$ m/s, at a pace of $\Delta U = 0.1$ m/s. As a comparison measurement, a few tests were repeated with the piezoelectric circuit opened, therefore not extracting energy from the structure.

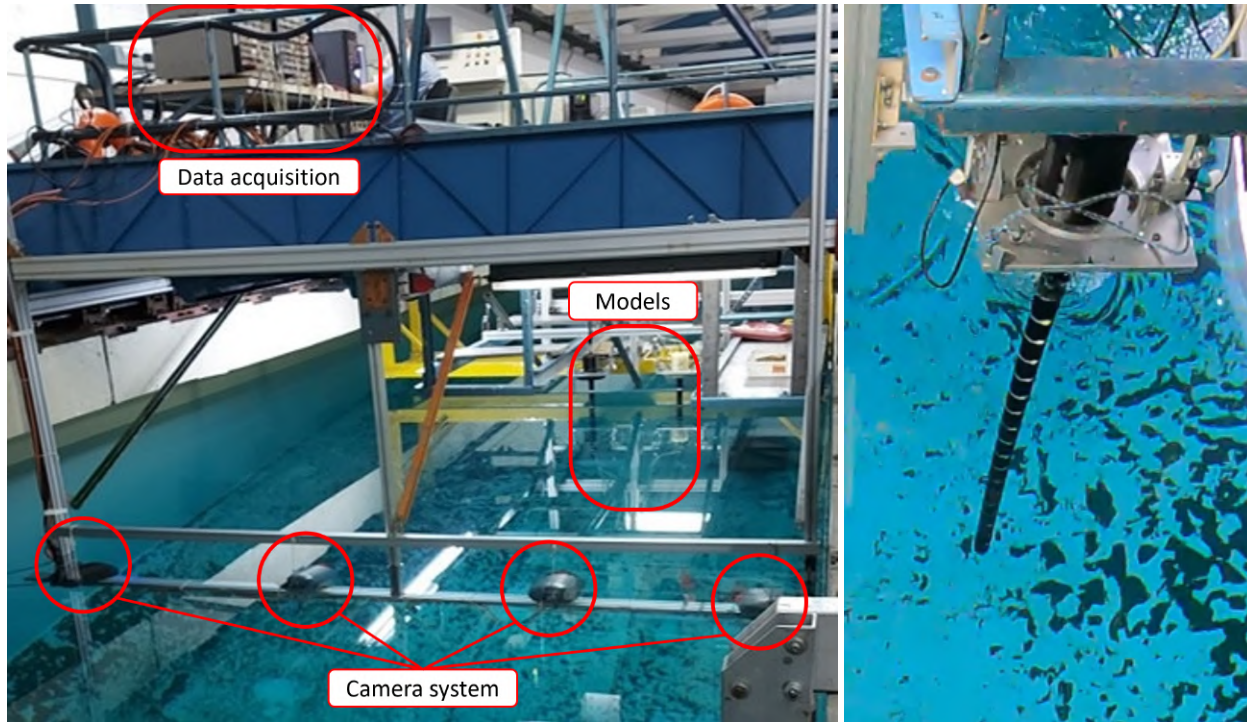


Figure 4. Experimental assembly in the IPT towing tank. Arrangement of the towing car (left) and cantilevered model attached to the car structure in the water channel (right).

3. RESULTS AND DISCUSSION

The current section presents the results obtained from the tests conducted with a closed electric circuit, extracting electric power from the system. The discussion focuses on several key aspects, including the displacements of the model and the respective trajectories, the corresponding amplitudes and frequency spectra observed. The electric tension measured and estimatives of the power harvested are also addressed.

Initially, the raw data undergoes an *ad hoc* pre-processing algorithm that recreates lost signals and interpolates the data to a more refined discretization along the model (see Defensor Fo *et al.* (2023); Vernizzi *et al.* (2023)). The resulting time series of movement and the corresponding trajectories of the model's tip are then presented in Fig. 5. These trajectories are showcased for selected test velocities, providing a visual representation of the model's behaviour during the experiments. The displacements are made dimensionless by the diameter of the cylinder, and the reduced velocity is defined by the natural frequency of the first transversal mode as $Ur_1 = U/f_{y1}D$. Notably, the "eight-shaped" trajectory observed in the presented figures is a distinctive characteristic of the dual resonance phenomenon commonly associated with VIV. This particular trajectory pattern emerges when the frequency relationships between the governing hydrodynamical parameters closely approximate a 2:1 ratio.

For each tested velocity, the amplitude of the steady state section of the time series was determined by considering the 10% highest peaks. The in-line displacement amplitude at the tip of the model, denoted as A_x^* , and the cross-wise displacement amplitude, denoted as A_y^* , are presented in Figure 6. It is also shown that when comparing these amplitudes with those obtained from tests conducted with an open electric circuit, minimal differences are observed, indicating that the presence of the harvesting system has negligible impact on the measured amplitudes. The in-line lock-in occurs in synchronization with the cross-wise direction at approximately $Ur_1 = 7.5$, attributed to the influence of orthotropic stiffness. Furthermore, the high energy branch is identified, starting at $Ur_1 = 10$ and yielding maximum amplitudes of $A_x^* = 0.5$ and $A_y^* = 1.6$.

¹Steady state is herein referred as the asymptotic behaviour of the dynamical system, as defined in Nayfeh (1995).

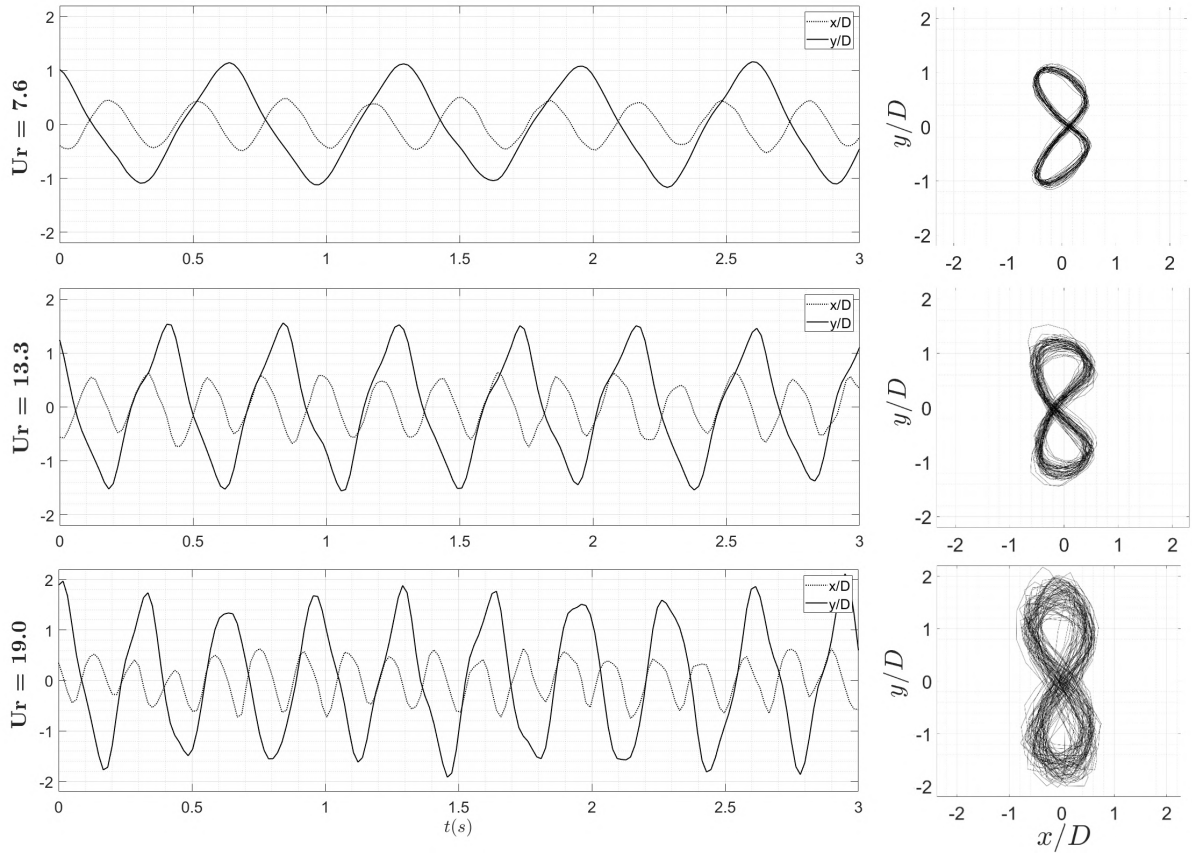


Figure 5. Time series of the displacements measured at the cantilever free end on the in-line and cross-wise directions and described trajectories, normalized by the cylinder diameter.

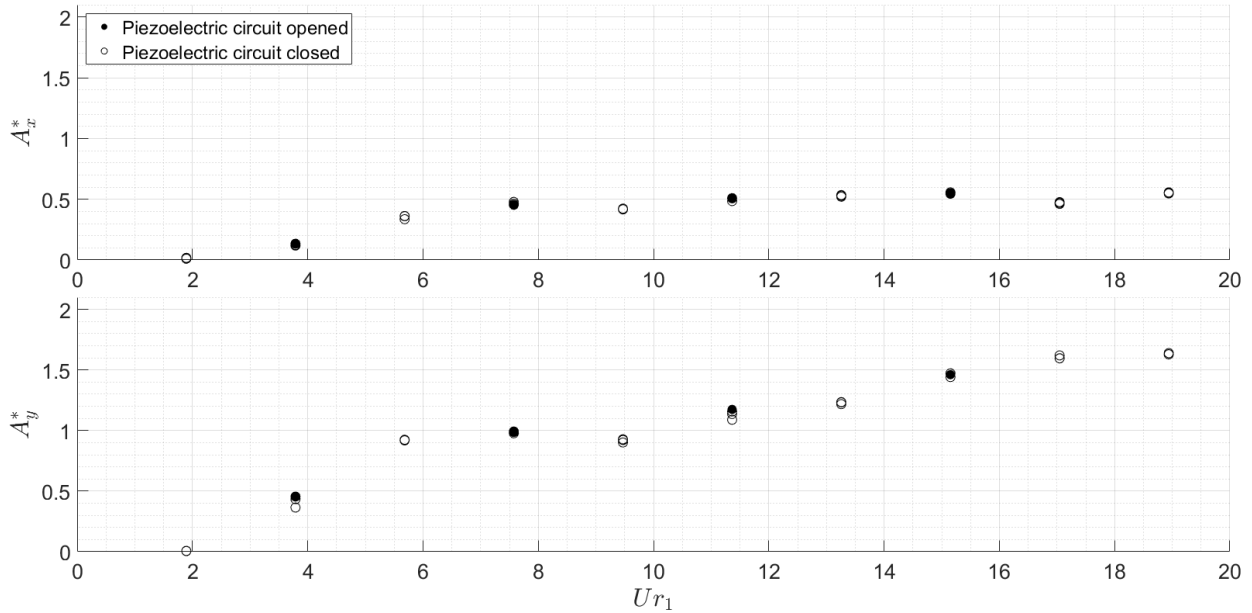


Figure 6. Dimensionless amplitudes of displacements for the cantilever end.

To further understand the dynamic response of the vibratory system, Galerkin's projection techniques were utilized for data analysis in the time domain, employing as modal functions the Euler-Bernoulli cantilever modes. Figure 7 presents the first two modal amplitudes for both transverse directions. This method reveals that the longitudinal response is predominantly captured within the first mode, while at higher reduced velocities, the transversal displacements show a second mode of vibration. In this case, the reduced velocity calculated for the second mode is around $Ur_2 = 3$, corresponding to the beginning of a new synchronization and the initial branch of the second mode.

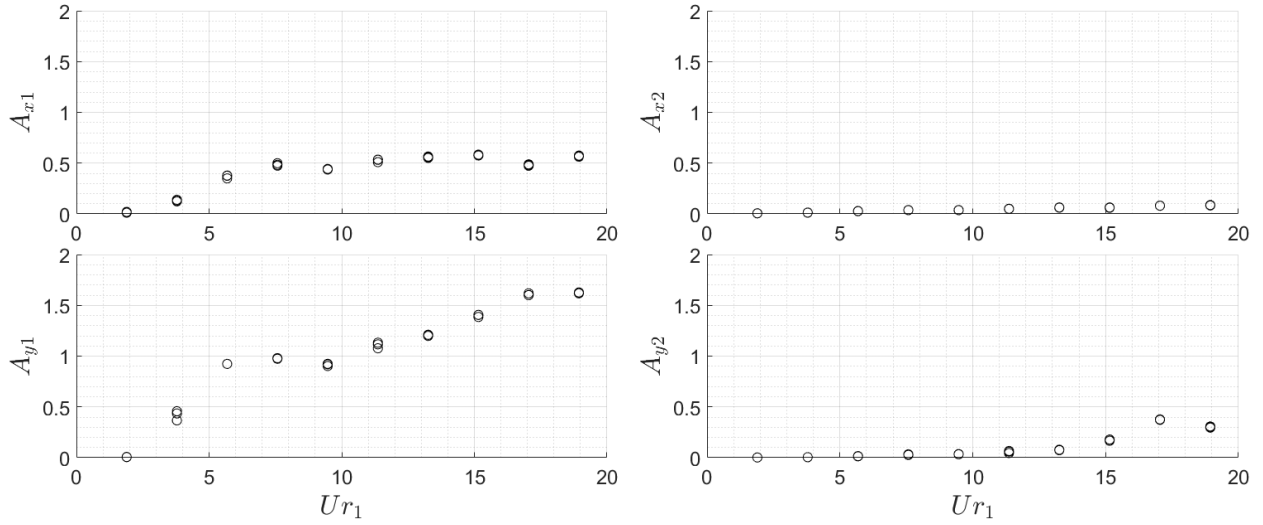


Figure 7. Modal amplitudes of displacements on in-line and cross-wise directions.

The frequency spectra for each mode on both directions are depicted in Fig. 8, where the red lines represent the natural frequencies in still water in its respective direction. For the first mode spectra, it is possible to see that the dominant frequency of the system on both directions is close to the natural frequencies, at reduced velocities from $Ur_1 = 5.7$ to $Ur_1 = 7.6$, which corresponds to the upper branch of the VIV phenomenon. For the second mode response, the frequencies get closer to the second natural frequency at high velocities, as it begins to enter the second mode lock-in at $Ur_2 = 3$.

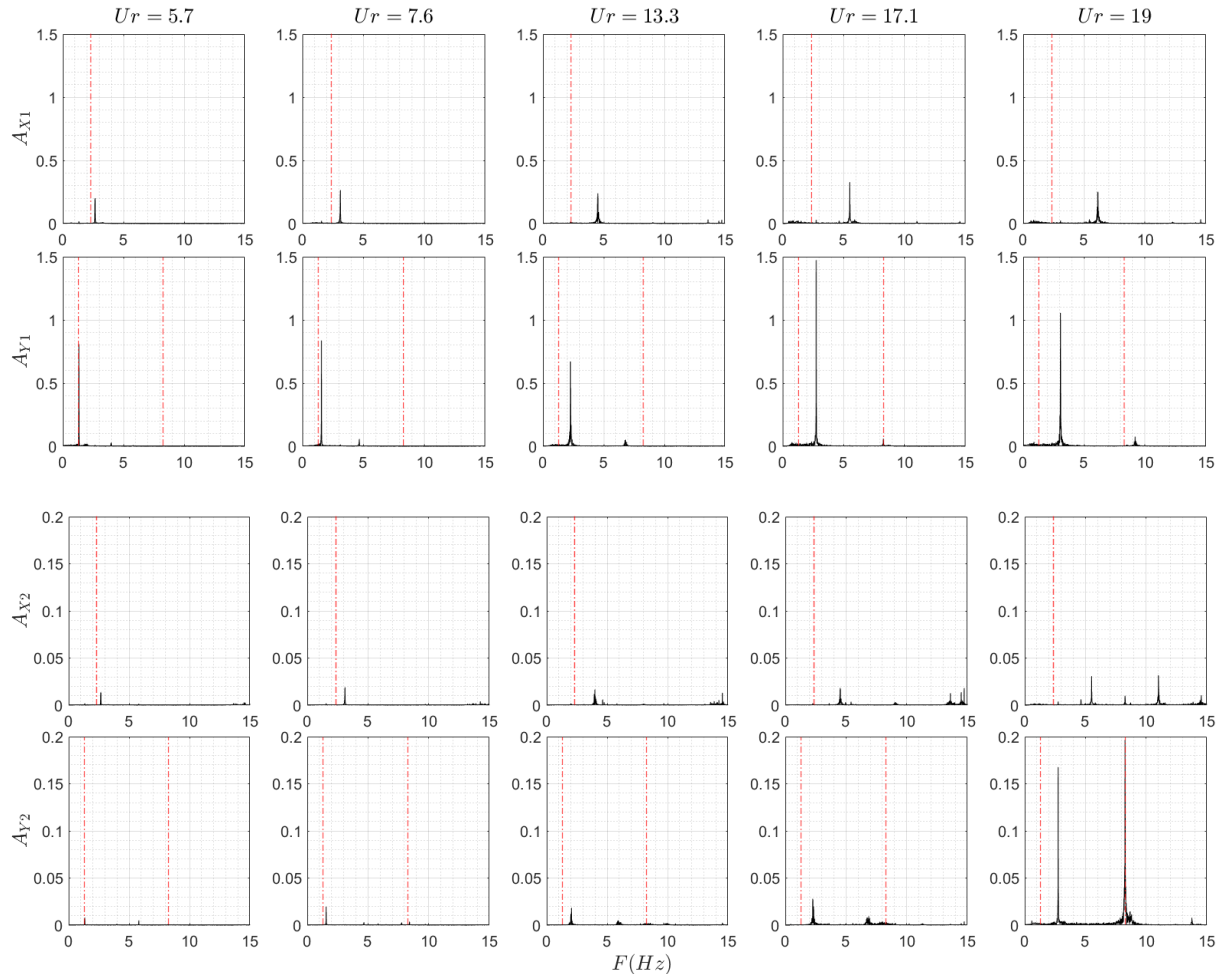


Figure 8. Frequency spectra of the modal amplitudes, natural frequencies in still water highlighted.

The electric tension output for one of the piezoelectric circuits is depicted as function of time in Fig. 9. The time series exhibit the presence of multiple frequency components, highlighting the non-harmonic nature of the signal in contrast to the almost harmonic displacement time series.

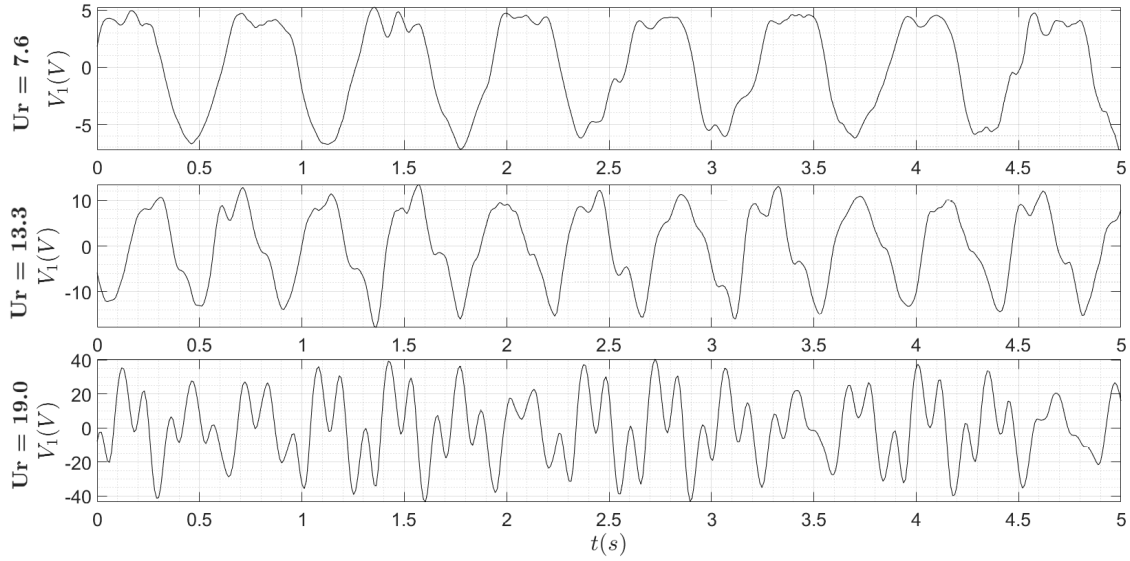


Figure 9. Time series for piezoelectric tension output.

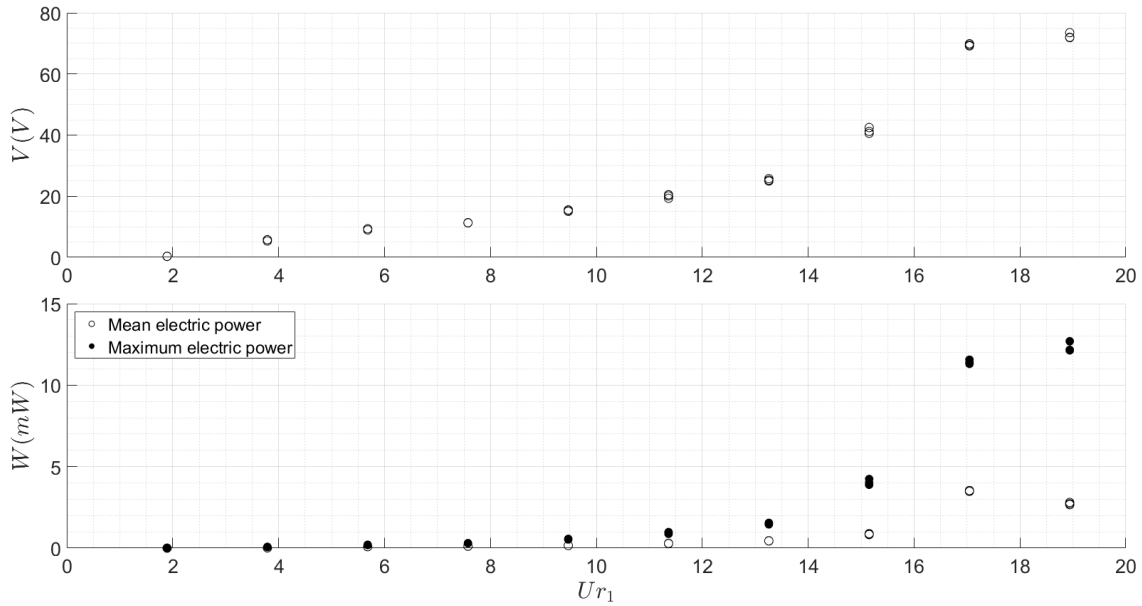


Figure 10. Electric tension and estimated power harvested.

The estimation of the electric power harvested by the system was determined using two different methods. Firstly, the maximum power value was calculated for each velocity by considering the peaks of the tension time series, using the expression $W_{max} = V^2/R$. Secondly, the steady state window was analysed to calculate the mean electric power by evaluating the work over time from the expression

$$W_m = \left(\int_{t_0}^{t_1} \frac{V^2}{R} dt \right) / (t_1 - t_0). \quad (1)$$

The results of these calculations, adding the values obtained for both circuits, are shown in Fig. 10, illustrating the total electric tension output of the system and the corresponding total electric power harvested estimated by both methods. The maximum power harvested reaches up to $W_{max} = 12.7$ mW, while the mean power is estimated to be $W_m = 3.5$ mW.

4. CONCLUDING REMARKS

The experimental study presented in this paper explored the potential of harnessing energy from VIV using a cantilevered cylinder with piezoelectric components, and the viability of extracting electrical power from the high-energy branch observed in VIV experiments with this specific configuration. The analysis of the displacements, trajectories, and frequency spectra provided valuable insights into the dynamic behaviour of the system.

The occurrence of a high energy branch for high reduced velocities was confirmed, obtaining maximum transversal amplitude of $A_y^* = 1.6$. By employing Galerkin's projection techniques, the dynamic response of the vibratory system was further understood, corroborating the presence of distinct modes in the high energy branch, and a rich frequency spectrum that can be explored. The electric tension output of the piezoelectric circuits exhibited a multi-frequency nature, indicating the complex electrical response of the system. The estimation of the electric power harvested from the system using two different methods demonstrated a maximum power output of $W_{max} = 12.7$ mW and a mean power output of $W_m = 3.5$ mW.

Overall, this experimental investigation serves as a proof-of-concept study, showcasing the potential of converting vibratory energy into electrical energy using the high-energy branch observed in VIV experiments with the proposed configuration. The findings contribute to the understanding of the system dynamics and provide a foundation for further optimization of energy conversion systems.

5. ACKNOWLEDGEMENTS

L. Madi and W. Defensor Fo acknowledge their PhD scholarships, supported by the CAPES social demand, through the Graduate Program in Naval and Ocean Engineering (PPGEN). C.P. Pesce acknowledges the Brazilian National Council for Scientific and Technological Development for the research grant 307995/2022-4. Acknowledgements also to IPT for support given to L. Madi through its Young Talent Program. The Sao Paulo Research Foundation (FAPESP) thematic project 'Nonlinear Dynamics Applied to Engineering Systems', process 2022/00770-0, is also acknowledged.

6. REFERENCES

- Bernitsas, M.M., Raghavan, K., Ben-Simos, Y. and Garcia, E.M.H., 2006. "VIVACE (Vortex Induced Vibration Aquatic Clean Energy): A new concept in generation of clean and renewable energy from fluid flow". In *Proceedings of OMAE2006 - International Conference on Offshore Mechanics and Arctic Engineering*.
- Defensor Fo., W.A., Franzini, G.R. and Pesce, C.P., 2022. "An experimental investigation on the dual-resonance revealed in the VIV of flexible cantilevers with orthotropic bending stiffness". *Applied Ocean Research*, Vol. 126, p. 103263. doi:10.1016/j.apor.2022.103263.
- Defensor Fo, W.A., Pesce, C.P., Vernizzi, G. and Maciel, V.S.F., 2023. "Experimental insights on the dynamics of submerged flexible pipes discharging water in post-critical regime". In *Proceedings of the XIX International Symposium on Dynamic Problems of Mechanics*. ABCM. doi:10.26678/abcm.diname2023.din2023-0115.
- Fujarra, A., Pesce, C., Flemming, F. and Williamson, C., 2001. "Vortex-induced vibration of a flexible cantilever". *Journal of Fluids and Structures*, Vol. 15, pp. 651–658.
- Han, P., Huang, Q., Pan, G., Qin, D., Wang, W., Gonçalves, R.T. and Zhao, J., 2023. "Optimal energy harvesting efficiency from vortex-induced vibration of a circular cylinder". *Ocean Engineering*, Vol. 282, p. 114869. doi:10.1016/j.oceaneng.2023.114869.
- Han, P., Pan, G., Zhang, B., Wang, W. and Tian, W., 2020. "Three-cylinder oscillator under flow: Flow induced vibration and energy harvesting". *Ocean Engineering*, Vol. 211, p. 107619. doi:10.1016/j.oceaneng.2020.107619.
- Khalak, A. and Williamson, C.H.K., 1999. "Motions, forces and modes transitions in vortex-induced vibration at low reynolds number". *Journal of Fluids and Structures*, Vol. 13, pp. 813–851.
- Nayfeh, A.H., 1995. *Applied nonlinear dynamics*. Wiley. ISBN 0471593486.
- Sarpkaya, T., 2004. "A critical review of the intrinsic nature of vortex-induced vibrations". *Journal of Fluids and Structures*, Vol. 19, pp. 389–447.
- Shan, X., Deng, J., Song, R. and Xie, T., 2017. "A piezoelectric energy harvester with bending–torsion vibration in low-speed water". *Applied Sciences*, Vol. 7, No. 2, p. 116. doi:10.3390/app7020116.
- Song, R., Shan, X., Lv, F., Li, J. and Xie, T., 2015. "A novel piezoelectric energy harvester using the macro fiber composite cantilever with a bicylinder in water". *Applied Sciences*, Vol. 5, No. 4, pp. 1942–1954. doi:10.3390/app5041942.
- Sun, H., Ma, C., Kim, E.S., Nowakowski, G., Mauer, E. and Bernitsas, M.M., 2017. "Hydrokinetic energy conversion by two rough tandem-cylinders in flow induced motions: Effect of spacing and stiffness". *Renewable Energy*, Vol. 107, pp. 61–80. doi:10.1016/j.renene.2017.01.043.
- Vernizzi, G.J., Maciel, V.S.F., Defensor Fo., W.A., Orsino, R.M.M., Franzini, G.R. and Pesce, C.P., 2023. "Dynamic small-scale riser model experiments: a physics-based algorithm to recover lost measurements from optical tracking systems." In *Proceedings of the 42nd International Conference on Ocean, Offshore and Arctic Engineering - OMAE*

2023. Melbourne, Australia.

Williamson, C.H.K. and Govardhan, R.N., 2004. “Vortex-induced vibrations”. *Annual Review of Fluids Mechanics*, Vol. 36, pp. 413–455.

Zhao, J., Thompson, M.C. and Hourigan, K., 2022. “Damping effect on transverse flow-induced vibration of a rotating circular cylinder and its implied energy harvesting performance”. *Physical Review Fluids*, Vol. 7, No. 2, p. 023905. doi:10.1103/physrevfluids.7.023905.

7. RESPONSIBILITY NOTICE

The authors are solely responsible for the printed material included in this paper.